ChemComm

Accepted Manuscript

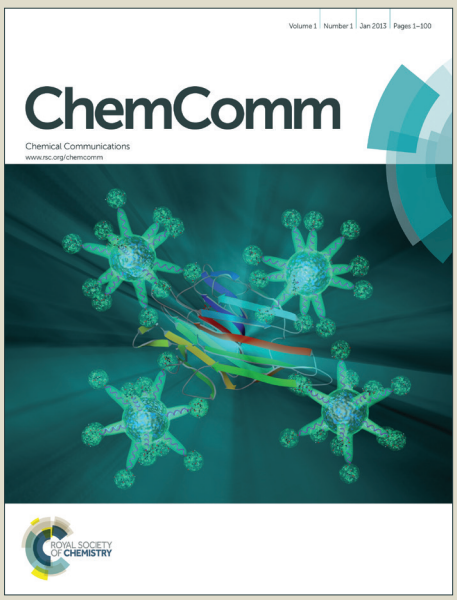

ROYAL SOCIETY OF CHEMISTRY

www.rsc.org/chemcomm

Journal Name

RSCPublishing

COMMUNICATION

Layered structures and nanosheets of pyrimidinethiolate coordination polymers

Cite this: DOI: 10.1039/xoxxoooooox

P. J. Beldon, [a] S. Tominaka,[ab] P. Singh,[c] T. Saha Dasgupta,[c] E. G. Bithell[a] & A. K. Cheetham,[a]

Received ooth January 2012,
Accepted ooth January 2012

DOI: 10.1039/xoxxoooooox

www.rsc.org/

We report the synthesis, crystal structure and exfoliation of a new member of an important family of layered compounds: lamellar pyrimidinethiolate coordination polymers. Conductivity measurements and DFT calculations of iron(II) pyrimidine-2-thiolate show that this material and a related compound are insulators.

Lamellar materials, with covalent connectivity in two dimensions and only weak van der Waals forces between the layers, can be exfoliated to give a suspension of nanosheets.[1] This opens routes to processing these materials in solution[2], depositing films[3] and studying the properties of single-layer nanosheets.[4] A wide range of lamellar materials can be exfoliated, such as graphene,[5,6] inorganic chalcogenides[7] and, more recently, coordination polymers.[8–10] The versatility of coordination polymers and the ability to tune their properties makes them attractive additions to the range of two-dimensional materials.

Pyrimidinethiolate compounds first attracted attention because the ligand adopts a wide range of coordination modes.[11–15] In 2001, a lamellar coordination polymer, nickel(II)pyrimidine-2-thiolate was reported to be electronically conducting.[16] Since then, the interest into these compounds has increased due to the expectation that the relatively expanded orbitals of sulfur will provide a good pathway for electronic conductivity between the metals and ligands.[17–19] This is part of a growing effort to synthesise conducting coordination polymers.[20–22] We revisited the pyrimidine-2-thiolate system, motivated by the prospect of exfoliating nanosheets of this important class of coordination polymer.

We synthesised a new lamellar iron(II)-pyrimidine-2-thiolate coordination polymer, $[Fe(Py2th)_2]_n$, and using single-crystal X-ray diffraction (SC-XRD) found the compound to be isostructural with the previously reported nickel compound (Figure 1(a)). We successfully exfoliated this material by sonicating the crystals in ethanol, then leaving the suspension to stand for 18 hours to allow the larger particles to sediment out of suspension. After this time the suspension

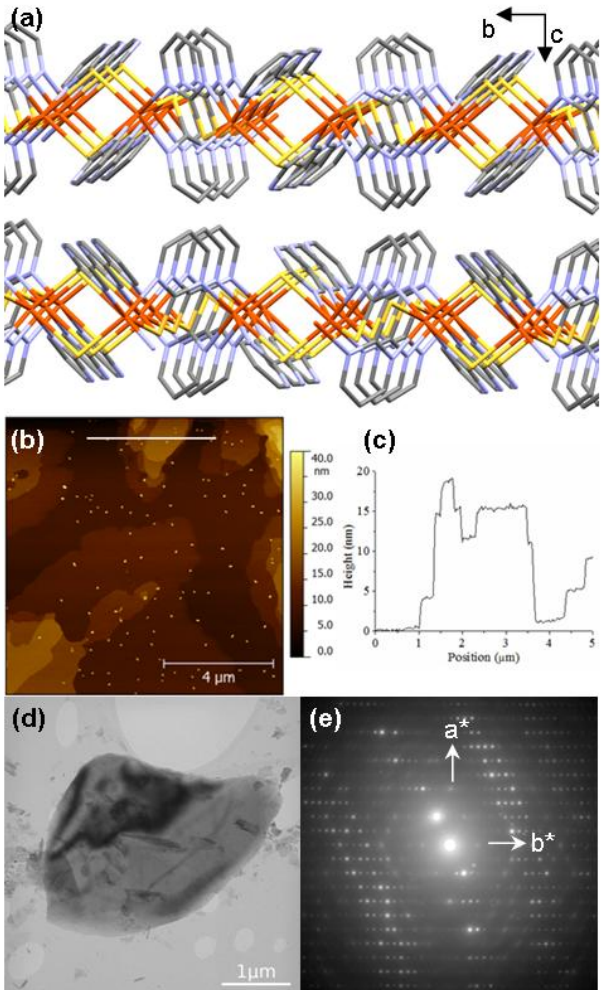

Figure 1 (a) Lamellar structure of $[Fe(Py2th)_2]_n$. Atoms are coloured: C, grey; N, blue; S, yellow; Fe, orange; hydrogen atoms have been omitted for clarity. (b) AFM image of nanosheets of $[Fe(Py2th)_2]_n$. (c) Height profile along the white line shown in (b). (d) TEM image of a cluster of nanosheets of $[Fe(Py2th)_2]_n$. (e) Electron diffraction pattern of the nanosheet shown in (d).

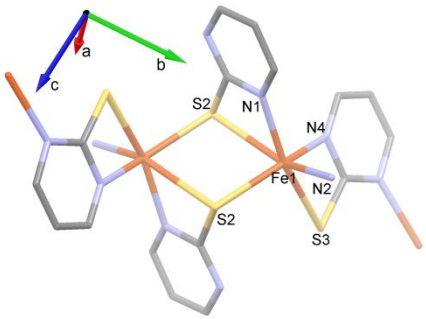

Figure 3 Coordination sphere of $[Fe(Py2th)_2]_n$ showing atom labels. C atoms are shown in grey. H atoms are omitted for clarity.

Table 1 – Structural data determined by single-crystal diffraction at 20°C

Bond	Bond length (Å)		Sum of Shannon radii (Å)	
	$[Fe(Py2th)_2]_n$	$[Ni(Py2th)_2]_n$	High spin Fe d^6	Low spin Fe d^6
Metal-N1	2.153	2.055		
Metal-N4	2.174	2.074	2.24	2.07
Metal-N2	2.215	2.142		
Metal-S2	2.4703	2.438		
Metal-S3	2.5480	2.452	2.62	2.45
Metal-S2	2.7828	2.593		

showed strong Tyndall scattering, indicating the presence of particles with a size on the order of hundreds of nm. The suspension was deposited onto substrates for characterisation by atomic force microscopy (AFM) and transmission electron microscopy (TEM). AFM shows that the nanosheets have a terraced morphology (Figure 1(b) & (c)). The terrace height was around 3.2 nm, corresponding to two unit cells (i.e. four covalently bound layers) per terrace, and no terraces corresponding to single lamellae were observed. The $[Fe(Py2th)_2]_n$ nanosheets were examined by TEM. Electron diffraction patterns of the nanosheets match the pattern calculated for $[Fe(Py2th)_2]_n$, exfoliated along the (001) planes (Figure 1(d) & (e)).

In the $[Fe(Py2th)_2]_n$ crystals, the iron(II) ion sits in a distorted octahedral coordination environment with 3 sulfur and 3 nitrogen donors (**Figure 2**). Under such conditions, Fe d^6 may have a high spin or low spin configuration. A comparison of the bond lengths to the expected ionic radii (Shannon radii[23,24]) shows that Fe is in the high spin d^6 state (Table 1). As a result of the distorted metal site, in the Fe compound there is a slight elongation of the b-axis (within the lamellae) and a slight contraction along the c-axis (perpendicular to the lamellae) compared to the Ni compound.

To better understand the electronic structure of these materials we carried out spin-polarised density functional theory (DFT) calculations. The ground state configuration of $[Fe(Py2th)_2]_n$ was found to be d^6 high-spin (in agreement with the crystal chemistry argument) with the HOMO-LUMO gap formed between the occupied d_{xy} and unoccupied d_{xz} state, both in the down spin channel (see Δ, **Figure 3**(b)). For $[Ni(Py2th)_2]_n$, the configuration was calculated to be d^8 high-spin with the highest occupied states being the doubly degenerate e_g (spin up) states. The lowest unoccupied states are the e_g (spin down) states, which lie 0.7eV higher in energy.

The partial density of states and the charge density plots calculated for $[Fe(Py2th)_2]_n$ and $[Ni(Py2th)_2]_n$ at 0 K (Figure 3) show that the contribution of the states close to the Fermi energy, i.e. those relevant for conduction, are primarily localized at metal centres with small weights at neighbouring pyrimidine rings. For good electronic

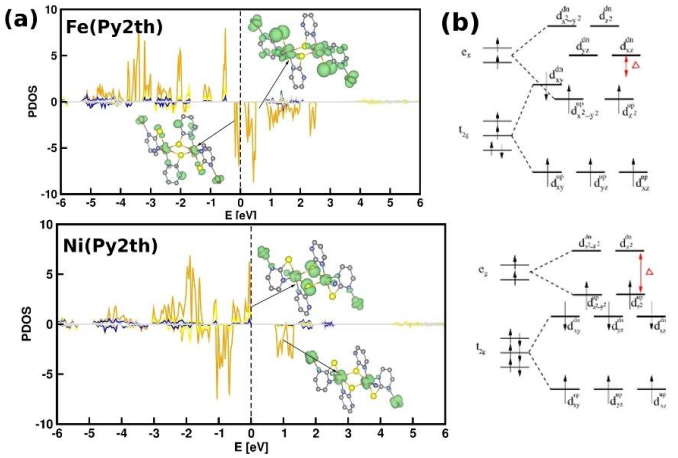

Figure 2 (a) Spin-polarised density of states for $[Fe(Py2th)_2]_n$ and $[Ni(Py2th)_2]_n$. The insets show charge density plots, corresponding to states near the Fermi energy. The small band width and the limited mixing of states across different elements, indicate the localized character of the materials. (b) Crystal field splitting of the metal d states and their occupancies for $[Fe(Py2th)_2]_n$ and $[Ni(Py2th)_2]_n$. Δ indicates the gap between filled/unfilled spin states.

communication between metal dimers, one would expect rather large weights on the pyrimidine rings, acting as a pathway to connect different metal centres in the material. The calculated band structures for $[Fe(Py2th)_2]_n$ and $[Ni(Py2th)_2]_n$ are given in ESI Figure S5. The levels close to the Fermi energy are metal-centred orbitals and have very flat bands indicating that the electrons have a localized character. These observations suggest that, although the energy gap between the filled and unfilled states is small ($[Fe(Py2th)_2]_n$: 0.14 eV; $[Ni(Py2th)_2]_n$: 0.7 eV), the materials are better classified as insulators than semiconductors. As the gap is between highly localized states, rather than between delocalized bands, it is more appropriate to call the energy gap a HOMO-LUMO gap than to call it a band gap.

These observations led us to revisit the conductivity measurements reported previously. The $[Ni(Py2th)_2]_n$ crystals synthesized using the reported procedure were a mixture of green plate-like crystals with a tiny amount of brown crystals, (ESI Figure S1) and so we optimized the conditions to obtain pure samples of the green crystals and large amounts of the brown crystals. Zhao et al. reported obtaining dark-brown, sheet-like crystals (Pbca a = 7.8860 Å, b = 15.5844 Å, c = 16.2399 Å at room temperature); however, our green plate-like crystals match this structure. The brown needle-like crystals have a new structure, judged from cell parameters obtained from SC-XRD (P21/c a=3.6580 Å, b=6.7100 Å, c=21.560 Å, β=90.64°). Unfortunately we were unable to fully solve the structure of the brown phase due to the small size of the crystals and extent of disorder; however, a partial solution from SC-XRD suggests that the compound forms one-dimensional chains.

Conductivity measurements were made on single crystals of the three materials at 30°C using our setup recently reported.[25] In all cases, even at higher temperatures (60°C and 90°C), the resistance of the crystals was higher than the apparent resistance of the blank measurement. Given this observation and measurements of the crystal size by optical microscopy, we can place an upper bound of the conductivity of the materials (Table 2). In order to screen for the presence of highly conductive directions, we performed conductivity measurements on pressed-powder pellets. The powder

measurements also serve to confirm that defects or grain boundaries introduced during grinding do not have a positive influence on the conductivity. The pressed-pellet experiments gave a measureable current, thanks to the larger cross-section of the sample, and the conductivities (Table 2) were estimated from fitting the impedance data to an equivalent circuit (ESI Figure S3(d)). Given the low values of the conductivity (approx. 10^{-12} S cm^{-1}), we believe these materials are best characterised as insulators.

Table 2 - Conductivities found by AC impedance

Material	Upper bound of single crystal conductivity (S cm^{-1} at 30°C)	Powder conductivity (S cm^{-1} at 30°C)
$[Ni(Py2th)_2]_n$	8×10^{-10}	4.5×10^{-13}
$[Fe(Py2th)_2]_n$	3×10^{-11}	2.0×10^{-12}
Brown phase	1×10^{-9}	2.2×10^{-13}

The discrepancy between our results and the previous report could be due to the presence in the previously reported samples of an impurity that acts as a dopant or is itself conducting. In the previous report, the colour was reported as dark brown, potentially mis-assigned due to a coloured impurity or due to the presence of a mixture of $[Ni(Py2th)_2]_n$ and the brown phase. Under the hydrothermal conditions used, one must consider the possibility of ligand decomposition or hydrolysis. We confirmed the colours of the reagents and $[Ni(Py2th)_2]_n$ by UV/Vis spectroscopy (ESI Figure S4). The $[Ni(Py2th)_2]_n$ spectrum matches well to a superposition of the spectra of the reagents, implying that the green colour of $[Ni(Py2th)_2]_n$ is due to metal-centred d-d transitions and ligand-ligand transitions. This observation indicates that there is little delocalisation throughout the material and reinforces the conclusion that the material is not conducting.

In summary, we have synthesised and characterised a lamellar coordination polymer $[Fe(Py2th)_2]_n$, which contains Fe(II) in a high spin d^6 configuration. DFT, conductivity measurements and UV/VIS spectroscopy were used to elucidate the electronic structure of $[Fe(Py2th)_2]_n$. Using sonication, $[Fe(Py2th)_2]_n$ can be exfoliated into nanosheets, which we have studied using AFM and TEM. Nanosheets of coordination polymers are valuable extensions to the scope of two-dimensional materials.

Notes and references

P.J.B thanks EPSRC for funding via Cambridge NanoDTC. P.S. and T.S.D. thank the INDO-SWEDISH project for financial support.

[a] Materials Science & Metallurgy, University of Cambridge, CB3 0FS, UK. E-mail: akc30@cam.ac.uk; Tel: +44 (0)1223 767061

[b] International Center for Materials Nanoarchitectonics (WPI-MANA), National Institute for Materials Science (NIMS), Ibaraki 305-0044, Japan.

[c] S.N. Bose National Centre for Basic Sciences, Block-JD, Salt Lake, Kolkata 700098, India

Electronic Supplementary Information (ESI) available: [experimental procedures, additional materials characterisation data and crystallographic information file (CIF) CCDC: 983822]. See DOI: 10.1039/c000000x/

1. J. N. Coleman, M. Lotya, A. O'Neill, S. D. Bergin, P. J. King, U. Khan, K. Young, A. Gaucher, S. De, R. J. Smith, I. V Shvets, S. K. Arora, G. Stanton, H.-Y. Kim, K. Lee, G. T. Kim, G. S. Duesberg, T. Hallam, J. J. Boland, J. J. Wang, J. F. Donegan, J. C. Grunlan, G. Moriarty, A. Shmeliov, R. J. Nicholls, J. M. Perkins, E. M. Grieveson, K. Theuwissen, D. W. McComb, P. D. Nellist, and V. Nicolosi, *Science*, 2011, **331**, 568–71.
2. A. O'Neill, U. Khan, and J. N. Coleman, *Chem. Mater.*, 2012, **24**, 2414–21.
3. M. Osada and T. Sasaki, *Adv. Mater.*, 2012, **24**, 210–28.
4. Z. Zeng, Z. Yin, X. Huang, H. Li, Q. He, G. Lu, F. Boey, and H. Zhang, *Angew. Chem. Int. Ed. Engl.*, 2011, **50**, 11093–7.
5. D. Li, M. B. Müller, S. Gilje, R. B. Kaner, and G. G. Wallace, *Nat. Nanotechnol.*, 2008, **3**, 101–5.
6. Y. Hernandez, V. Nicolosi, M. Lotya, F. M. Blighe, Z. Sun, S. De, I. T. McGovern, B. Holland, M. Byrne, Y. K. Gun'Ko, J. J. Boland, P. Niraj, G. Duesberg, S. Krishnamurthy, R. Goodhue, J. Hutchison, V. Scardaci, A. C. Ferrari, and J. N. Coleman, *Nat. Nanotechnol.*, 2008, **3**, 563–8.
7. C. N. R. Rao, H. S. S. Ramakrishna Matte, and U. Maitra, *Angew. Chem. Int. Ed. Engl.*, 2013, **52**, 13162–85.
8. P.-Z. Li, Y. Maeda, and Q. Xu, *Chem. Commun. (Camb).*, 2011, 8436–8.
9. J.-C. Tan, P. J. Saines, E. G. Bithell, and A. K. Cheetham, *ACS Nano*, 2012, **6**, 615–21.
10. A. Gallego, C. Hermosa, O. Castillo, I. Berlanga, C. J. Gómez-García, E. Mateo-Martí, J. I. Martínez, F. Flores, C. Gómez-Navarro, J. Gómez-Herrero, S. Delgado, and F. Zamora, *Adv. Mater.*, 2013, **25**, 2141–6.
11. I. A. Latham, G. J. Leigh, C. J. Pickett, G. Huttner, I. Jibrill, and J. Zubieta, *J. Chem. Soc. Dalt. Trans.*, 1986, 1181–7.
12. S. G. Rosenfield, H. P. Berends, L. Gelmini, D. W. Stephan, and P. K. Mascharak, *Inorg. Chem.*, 1987, **26**, 2792–7.
13. A. Eichhöfer and G. Buth, *Eur. J. Inorg. Chem.*, 2005, **2005**, 4160–7.
14. Z.-M. Hao, J. Wang, and X.-M. Zhang, *CrystEngComm*, 2010, **12**, 1103-9.
15. J. Zhang, S. Gao, X.-X. Zhang, Z.-M. Wang, and C.-M. Che, *Dalt. Trans.*, 2012, **41**, 2626-31.
16. Y. Zhao, M. Hong, Y. Liang, R. Cao, J. Weng, S. Lu, and W. Li, *Chem. Commun.*, 2001, **28**, 1020–1.
17. A. Gallego, O. Castillo, C. J. Gómez-García, F. Zamora, and S. Delgado, *Inorg. Chem.*, 2012, **51**, 718–27.
18. D. L. Turner, T. P. Vaid, P. W. Stephens, K. H. Stone, A. G. DiPasquale, and A. L. Rheingold, *J. Am. Chem. Soc.*, 2008, **130**, 14–5.
19. A. Walsh, *Proc. R. Soc. A Math. Phys. Eng. Sci.*, 2011, **467**, 1970–1985.
20. S. Takaishi, M. Hosoda, T. Kajiwara, H. Miyasaka, M. Yamashita, Y. Nakanishi, Y. Kitagawa, K. Yamaguchi, A. Kobayashi, and H. Kitagawa, *Inorg. Chem.*, 2009, **48**, 9048–50.
21. Y. Kobayashi, B. Jacobs, M. D. Allendorf, and J. R. Long, *Chem. Mater.*, 2010, **22**, 4120–2.
22. M. Ballesteros-Rivas, A. Ota, E. Reinheimer, A. Prosvirin, J. Valdés-Martinez, and K. R. Dunbar, *Angew. Chem. Int. Ed. Engl.*, 2011, **50**, 9703–7.
23. R. D. Shannon and C. T. Prewitt, *Acta Crystallogr. Sect. B Struct. Crystallogr. Cryst. Chem.*, 1969, **25**, 925–46.
24. R. D. Shannon, *Acta Crystallogr. Sect. A*, 1976, **32**, 751–67.
25. S. Tominaka, S. Henke, and A. K. Cheetham, *CrystEngComm*, 2013, **15**, 9400–7.